Formulation of photocleavable liposomes and the mechanism of their content release†

Binita Chandra,[a] Rajesh Subramaniam,[a] Sanku Mallik*[a] and D. K. Srivastava*[b]

Received 4th January 2006, Accepted 22nd February 2006
First published as an Advance Article on the web 29th March 2006
DOI: 10.1039/b518359f

In pursuit of designing photocleavable liposomes as drug delivery vehicles, we synthesized several amphiphilic lipids by connecting stearyl amine (as the non-polar tail) and charged amino acids (as polar heads) *via* the *o*-nitrobenzyl derivatives. The lipids containing Glu, Asp, and Lys amino acids were subjected to photocleavage reaction by UV light, and the overall spectral changes of the chromophoric *o*-nitrobenzyl conjugates were determined as a function of time. The experimental data revealed that the feasibility of the cleavage reaction, nature and magnitude of the spectral changes during the course of the cleavage reaction, and their overall kinetic profiles were dictated by the type of amino acid constituting the polar head groups. The cleavage reactions of the Asp and Glu containing lipids were found to be more facile than that of the lysine-containing lipid. Using these lipids, we formulated photocleavable liposomes, and investigated the photo-triggered release of an encapsulated (within the liposomal lumen) dye as a function of time. The kinetic data revealed that the release of the liposomal content conformed to a two-step mechanism, of which the first (fast) step involved the photocleavage of lipids followed by the slow release of the liposomal content during the second step. The overall mechanistic features intrinsic to the photocleavage of Asp, Glu and Lys containing *o*-nitrobenzyl conjugated lipids, and their potential applications in formulating liposomes (whose contents can be "unloaded" by the UV light) as drug delivery vehicles are discussed.

Introduction

Among drug carriers, liposomes have been considered to be an efficient drug delivery vehicle. Presently, there are 13 liposome-mediated drug delivery systems approved for the treatment of a variety of human diseases (*e.g.*, breast cancer, ovarian cancer, meningitis, fungal infections, leukemia, *etc.*).[1] In addition, the liposome-mediated delivery of about 30 other small molecule drugs, DNA fragments, and diagnostic compounds are currently at different stages of clinical trials.[1]

In liposome-mediated target-specific drug delivery systems, three features need to be taken into consideration: (i) appropriate coating of liposomes to circumvent their clearance by the reticuloendothelial system (RES), (ii) attachment of the target-specific recognition moiety (*e.g.*, antibodies, receptor agonist/antagonist), and (iii) incorporation of the triggering mechanism. Polyethylene glycol coating of liposomes precludes their recognition by the RES,[2] and attachment of receptor specific ligands ensures their adhesion to the target cell surface.[3] At the target sites, passive release of the liposome contents can take place by the fusion of liposomes with cell membranes.[4] But this process is too slow for effective drug release. In addition, the liposomal contents (*e.g.*, easily degradable drug molecules, nucleic acids, enzymes, *etc.*), entrapped by endosomes and subsequently exposed to the lysosomal system, are destroyed prior to eliciting their effects. These constraints could be circumvented by developing "triggered release methodology" of the liposomal contents. The triggering agents commonly employed are pH,[5] mechanical stress,[6] metal ions,[7] temperature,[8] light,[9] and enzymes.[10]

We recently demonstrated the triggered release of liposomal contents by a matrix metalloproteinase, MMP-9.[11] Since MMP-9 is overexpressed in a variety of cancerous tissues,[12] the overall methodology is likely to find applications in drug delivery. However, if the cancerous tissues do not overexpress MMP-9, this method cannot be used for triggering the release of liposomal contents. In order to develop a more general "triggered" release methodology, we noted that *o*-nitrobenzyl substituted compounds are easily cleaved by near-UV radiation.[13] This group is widely used in organic synthesis as a photolabile protecting group[14] and as a photocleavable linker in solid phase synthesis[15] because of its high photocleavage efficiency in the near-UV range (wavelength >320 nm). The above group has also been used for "caging" a variety of biologically important molecules such as ATP,[16] cAMP,[17] cGMP,[18] and neurotransmitters,[19] as well as in designing photo-prodrugs.[20] With these applications in mind, we recently synthesized a few *o*-nitrobenzyl group-containing lipids (with acidic amino acids as the polar head groups), and investigated their cleavage reactions in a preliminary manner.[21]

It should be mentioned that photolabile liposomes have been frequently formulated, in recent years, using various dithiane-based photocleavable lipids.[9] In these formulations,

[a]*Department of Pharmaceutical Sciences, North Dakota State University, Fargo, North Dakota, 58105, USA. E-mail: sanku.mallik@ndsu.edu; Fax: 701-231-8333; Tel: 701-231-7661*
[b]*Department of Chemistry, Biochemistry and Molecular Biology, North Dakota State University, Fargo, North Dakota, 58105. E-mail: dk.srivastava@ndsu.edu; Fax: 701-231-7884; Tel: 701-231-7831*

† Electronic supplementary information (ESI) available: spectra for the liposomal release studies incorporating the photocleavable lipids. See DOI: 10.1039/b518359f

photocleavable amphiphilic lipids are synthesized by interfacing a dithiane group between phosphocholine as the polar "head" groups and fatty acids as the non-polar "tails". Photopolymerization induced destabilization of liposomes and subsequent release of liposomal contents are also reported.[9] Although these lipids are well suited for formulating photocleavable liposomes, their synthetic schemes are rather elaborate and time consuming. In contrast, our syntheses of *o*-nitrobenzyl containing photocleavable lipids are fairly simple, and several variants of the head and tail groups could be easily incorporated to produce liposomes with diverse photo-triggered "unloading" features. Herein, we elaborate on the syntheses of selected *o*-nitrobenzyl group containing lipids, and investigate the influence of the oppositely charged polar head groups (contributed by Asp, Glu and Lys amino acids) on the spectral and kinetic features of the overall photocleavage reaction. We further demonstrate that these lipids are ideally suited for formulating photocleavable liposomes, and discuss the underlying mechanism of their content release.

Results

The amphiphilic lipids were synthesized by incorporating "charged" amino acids (*viz.*, Asp, Glu and Lys) as "head" groups and the alkyl chain of stearyl amine as the "tail" group. These groups were conjugated to the photocleavable *o*-nitrobenzyl moiety, such that the cleavage releases the polar head groups, resulting in the "unloading" of the liposomal content due to destabilization of the lipid domains. The structures of the synthesized lipids are shown in Fig. 1.

Scheme 1 summarizes the synthetic details of the lipids in Fig. 1. To synthesize these lipids, commercially available *p*-aminomethyl benzoic acid was trifluoroacetylated with trifluoroacetic anhydride to give the protected amine in 88% yield. This protected amine was subjected to regiospecific nitration at −10 °C with fuming nitric acid to give **2** in 92% yield. In the following two steps, the trifluoroacetyl group was efficiently replaced by a *t*-butyloxycarbonyl (Boc) group (**3**). Conjugation of the hydrophobic tail to the carboxylic acid moiety of **3** was performed by reaction with stearyl amine in presence of the peptide coupling reagents *O*-(benzotriazol-1-yl)-*N*,*N*,*N*′,*N*′ tetramethyluronium hexafluorophosphate (HBTU), and 1-hydroxybenzotriazole (HOBT). The Boc group was removed with 4 M HCl in dioxane. The resultant free amine **4** was then coupled to the acid groups of appropriately protected amino acids (aspartic acid, glutamic acid and lysine). In the final step, the acid-sensitive protecting groups were removed by treatment with trifluoroacetic acid to provide the lipids. The overall yields for all the steps were very good and the synthetic scheme is a significant improvement over that used by Nagasaki *et al.* in their synthesis of a similar lysine derivative.[22]

To ensure that our synthesized lipids underwent photolysis, and the overall process produced the expected intermediates, we determined the time course of the spectral changes upon irradiation of the individual lipid at appropriate wavelengths. In a typical experiment, an ethanolic solution of a lipid was irradiated for different time intervals, and the absorption spectra were immediately recorded. It was observed that the Asp-lipid and the Glu-lipid were cleaved upon irradiation at 365 nm, but the Lys-lipid required irradiation at 254 nm for efficient cleavage. Besides, there was a marked difference in the spectral and kinetic profiles of these lipids during the course of the photocleavage reaction.

Fig. 2 shows the time dependent spectral changes upon irradiation of Glu-lipid at 365 nm. Initially, Glu-lipid showed a pronounced spectral band around 245 nm and a shoulder band around 300 nm. Upon irradiation at 365 nm, the original shoulder peak appeared to split into two predominant peaks at 290 and 320 nm, with a "valley" at 304 nm. These peaks are apparent in the difference spectra (bottom left panel of Fig. 2), which were generated by subtracting the first spectrum (*i.e.*, the spectrum of Glu-lipid prior to irradiation). The difference spectral data reveal that as the irradiation time increases, the absorption bands at all the above wavelengths (*i.e.*, 290, 304, and 320 nm) increase and the overall spectral transition conforms to common isosbestic points. These spectral features led to the suggestion that no stable intermediary species (with distinct spectral characteristics) populated during the course of the photocleavage reaction. To further ascertain whether the spectral transitions of Fig. 2 involved kinetically predictable (metastable) intermediates, we analyzed the time dependent increase in absorptions at 290 nm, 304 nm, and 320 nm, respectively. The right panels of Fig. 2 show the time slices of the spectral data at the above wavelengths. These kinetic data were best fitted by the single exponential rate equation, with rate constants at 290, 304, and 320 nm of 0.36 ± 0.014, 0.32 ± 0.009, and 0.33 ± 0.015 min^{-1}, respectively. The solid smooth lines on the right hand (different wavelength) panels of Fig. 2 are the calculated lines for the above rate constants. Note a marked similarity in the above rate constants, attesting to the fact that

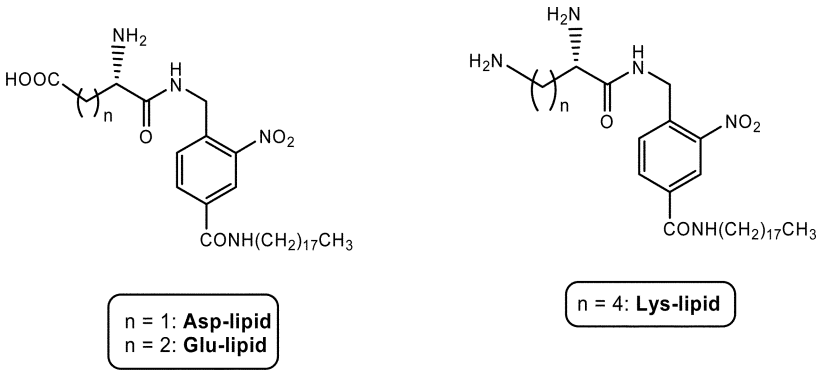

Fig. 1 Structures of the synthesized photocleavable lipids.

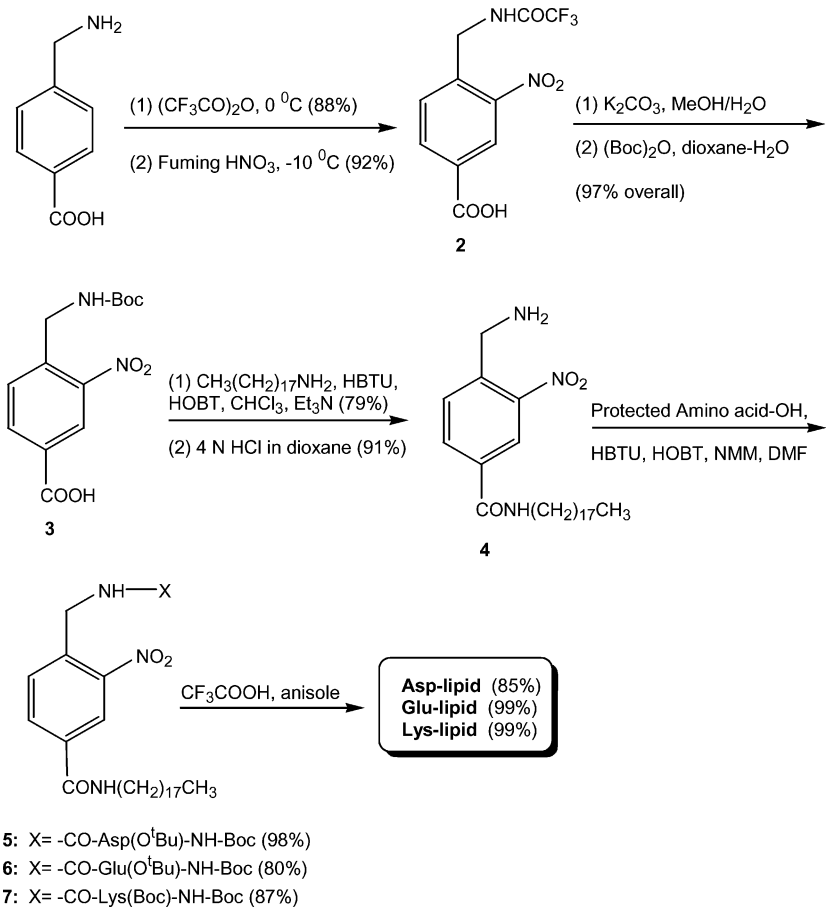

Scheme 1 The syntheses of the photocleavable lipids.

the spectral transition during the course of the photocleavage of Glu-lipid proceeded without the formation of any spectral distinct intermediary species.

To ascertain whether the spectral and/or kinetic profiles for the photocleavage of Asp-lipid are similar or different than those of Glu-lipid, we performed the photocleavage reaction of the former lipid exactly under the experimental conditions of Fig. 2. It was observed that the spectral changes during the course of photocleavage of Asp-lipid were remarkably the same as those observed with Glu-lipid. The only slight difference was the magnitude of the rate constants, derived from the spectral changes at 290, 304, and 320 nm, during the course of the photocleavage of Asp-lipid. The values for the photocleavage of Asp-lipid were determined to be 0.45 ± 0.024, 0.40 ± 0.026, and 0.43 ± 0.030 min^{-1} at 290, 304, and 320 nm, respectively. Since these kinetic parameters are not significantly different than those derived from the photocleavage of Glu-lipid, we conclude that the difference in the side chains of polar head groups (contributed by Glu *versus* Asp amino acids) has practically no influence on the spectral profiles and their associated rate constants during the photocleavage reaction. To avoid repetition of similar spectral and kinetic profiles, we provide the photocleavage data of Asp-lipid as Electronic Supplementary Information (Fig. S1)† of this journal.

Unlike the marked similarities in the spectral and kinetic profiles during the course of the photocleavage of Glu- and Asp-lipids, Lys-lipid exhibited quite different behavior. We first noted that Lys-lipid was not being readily photocleaved upon exposure to 365 nm UV light, the source which was adequate for the photocleavage of both Glu- and Asp-lipids. The photocleavage of Lys-lipid required exposure of the sample to a 254 nm (a higher energy) UV light source. Apparently, the presence of the "basic" head group (contributed by the ε-amino group of lysine) in Lys-lipid, somehow, thermodynamically and/or kinetically impairs the photocleavage reaction. The question arose whether or not the presence of the basic head group of Lys in Lys-lipid would yield relatively different types of spectral and kinetic profiles *vis a vis* those observed with Glu- and Asp-lipids. To ascertain this, we performed the photocleavage reaction of Lys-lipid exactly under the experimental conditions of Glu-lipid and Asp-lipid, except for using a 254 (instead of 365) nm UV light source. Fig. 3 (top left and bottom left panels) shows the time dependent spectral data during the course of the photocleavage of Lys-lipid. These spectral data appear significantly different than those obtained during the course of cleavage of Glu- (Fig. 2) and Asp-(ESI Figure S1†) lipids. The spectral data of Fig. 3 reveal that even prior to the onset of the cleavage process, the spectrum of Lys-lipid is significantly different those of Glu- and Asp-lipids. Although the major absorption peak of Lys-lipid at 245 nm is qualitatively similar to those observed with Glu- and Asp-lipids, the broad, less-resolved shoulder peak around 300 nm is unique for this lipid. A further difference is a spectral feature that started to emerge during the time dependent photocleavage reaction of Lys-lipid *vis a vis* Glu- and Asp-lipids.

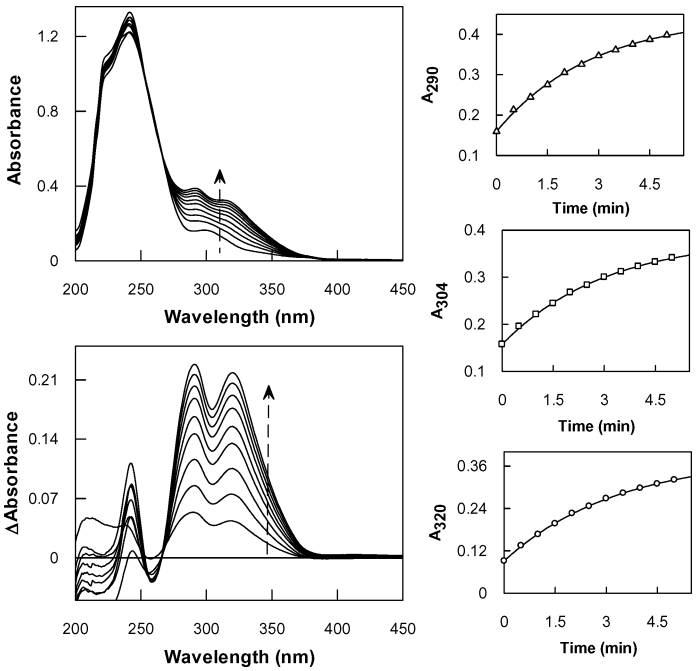

Fig. 2 Time dependent spectral changes upon photocleavage of Glu-lipid. The difference spectra (*i.e.*, spectra at different time intervals minus the zero time spectrum) are shown just below the main spectra. The time slices of the spectral changes at 290, 304 and 320 nm are shown on the right, and the solid smooth lines are the best fit of the data according to the single exponential rate equation with rate constants of 0.36 ± 0.014, 0.32 ± 0.009, and 0.33 ± 0.015 min^{-1} at 290, 304, and 320 nm, respectively.

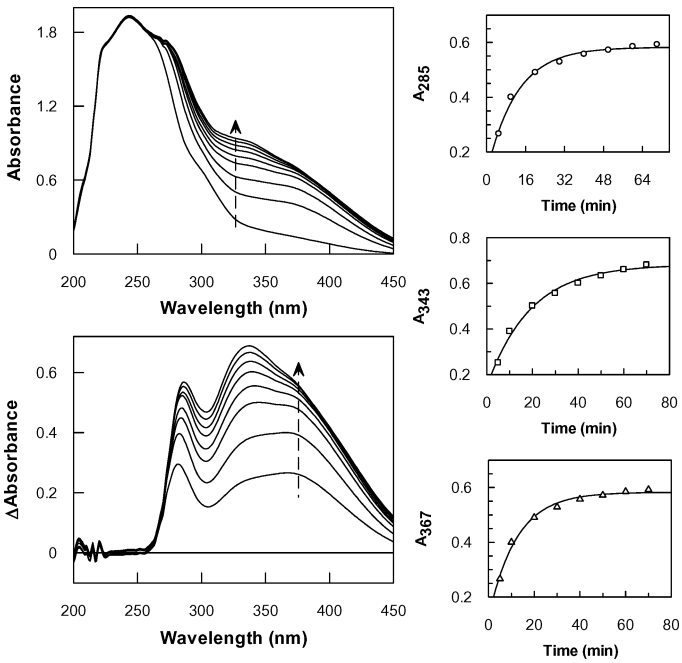

Fig. 3 Time dependent spectral changes upon photocleavage of Lys-lipid. The difference spectra (*i.e.*, spectra at different time intervals minus the zero time spectrum of each panel) are shown just below the main spectra. The time slices of the spectral changes at 285, 343 and 367 nm are shown on the right, and the solid smooth lines are the best fit of the data according to the single exponential rate equation with rate constants of 0.06 ± 0.0011, 0.05 ± 0.0010, and 0.08 ± 0.0012 min^{-1} at 285, 343, and 367 nm, respectively.

In the case of Lys-lipid, the 290 nm band is slightly blue shifted to 285 nm, but the 314 nm band is significantly red shifted to 343 nm, with emergence of another shoulder band at 367 nm. In addition, neither the peak around 245 nm nor the negative peak around 252 nm were evident in the difference spectra of Fig. 3. To our further interest, unlike Glu- and Asp-lipids, the spectral changes in the 280–400 nm region of Lys-lipid (during the course of photocleavage) were significantly broad and asymmetrical. A close inspection of the difference spectra (*i.e.*, the spectra of Lys-lipid at different times of photocleavage minus the uncleaved first spectrum; bottom left panel of Fig. 3) led us to select the spectral peaks at 285, 343, and 367 nm for undertaking kinetic analyses of the photocleavage reaction. The right hand panels of Fig. 3 show the time slices of spectral changes at the above wavelengths during the course of photocleavage of Lys-lipid. As observed with Glu- and Asp-lipids, the photocleavage data of Lys-lipid were also fitted by the single exponential rate equation. The solid smooth lines on the right hand panels of Fig. 3 are the nonlinear regression analysis of the experimental data for the rate constants 0.06 ± 0.0011, 0.05 ± 0.0010, and 0.08 ± 0.0012 min^{-1} at 285, 343, and 367 nm, respectively. Note that these values are about one order of magnitude smaller than those observed for the photocleavage of the Glu- and Asp-lipids. Hence, even upon exposure to a high-energy source (*i.e.*, irradiation with a 254 nm UV lamp), Lys-lipid is resistant (compared to Glu- and Asp-lipids) to the photocleavage reaction.

The ultimate goal of synthesizing these photocleavable lipids was to utilize them for formulating liposomes for the triggered release of their contents upon exposure to light. Hence, having characterized the feasibility of photocleavage of acidic (*viz.*, Glu and Asp) and basic (Lys) amino acid head groups containing *o*-nitrobenzyl conjugated lipids, we incorporated them into liposomes. The liposomes were prepared in 25 mM HEPES buffer, pH = 7.0, using 1,2-disteroylglycero-3-phosphocholine (DSPC) as a major component (95 mol%) and individual photocleavable lipids as minor components (5 mol%), encapsulating carboxyfluorescein as the self-quenching[23] reporter dye in the liposomal lumen. The excess (unincorporated) dye was removed by gel filtration to yield liposomes, which were only loaded with the reporter dye (see the experimental section). A representative TEM picture of a liposome formulated by using Glu-lipid is shown as Figure S2 in the ESI.†

We determined the fluorescence excitation and emission maxima of liposome-encapsulated carboxyfluorescein as being equal to 495 and 527 nm, respectively (data not shown). It is known that upon release from liposomal lumen, the fluorescence emission intensity of carboxyfluorescein increases,[11,21] due to dilution induced de-quenching of the excited state of the dye.[23] Fig. 4A shows a representative set of fluorescence emission spectra ($\lambda_{ex} = 495$ nm) for the release of carboxyfluorescein upon irradiating liposomes containing the Glu-lipid at 365 nm for different time intervals. A control experiment was performed in which the liposome solution was not irradiated, but the fluorescence spectra were recorded at corresponding time intervals (data not shown). From the spectral data of Fig. 4A, we extracted the time dependent increase in the fluorescence emission intensity (due to release of the liposome encapsulated carboxyfluorescein to the exterior media) at 518 nm.

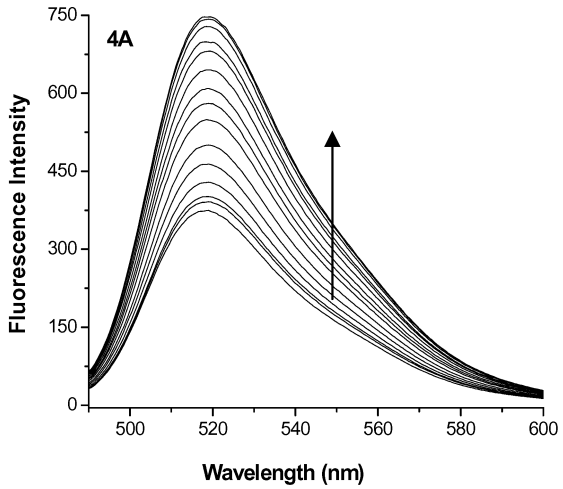

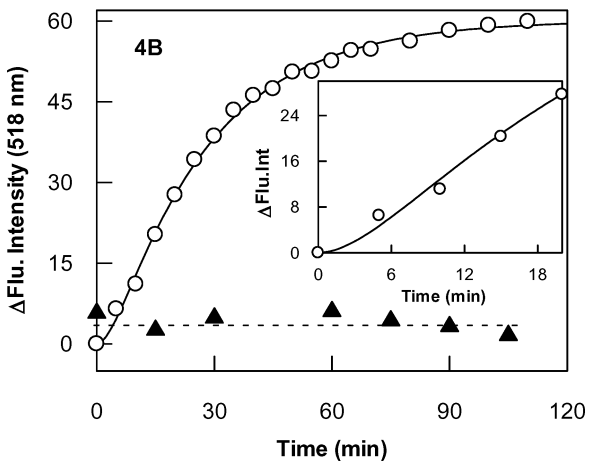

Fig. 4 Spectral and kinetic profiles for the release of carboxyfluorescein upon irradiation of Glu-lipid. **A**: Fluorescence emission spectra (λ_{ex} = 480 nm) as a function of irradiation time at 365 nm. **B**: The change in fluorescence intensity (ΔF_{518}/nm) as a function of time (open circle). The control experiment (solid triangle) was performed without irradiating the liposomes. The inset shows an expansion of the data at the initial time scale to show the lag phase. The solid smooth line is the best fit of the data for the photorelease of the liposomal content according to eqn. 2 with k_1 and k_2 values of 0.25 ± 0.018 and 0.04 ± 0.0024 min^{-1}, respectively.

These along with the control (in which the liposomes were not irradiated) data are shown as open circles and filled triangles, respectively, in Fig. 4B. Note that the fluorescence emission intensity of the reporter dye increases only when the liposomes are irradiated at 365 nm, and not when they are kept in the dark. Clearly, the irradiation of the carboxyfluorescein loaded liposomes at 365 nm results in the release of the dye due to the photocleavage of the resident Glu-lipid.

On examination of the time course for the release of carboxyfluorescein upon photocleavage of liposomes, it became evident that the overall kinetic profile involved an initial lag phase. The existence of such a lag phase is clear upon expanding the kinetic data for the initial time scale (see the inset of Fig. 4B), and it is more so in the case of photocleavage of Lys-lipid formulated liposomes (see Fig. 5). As will be discussed subsequently, the lag phase is associated with the photocleavage of liposomal lipids, resulting in the destabilization of lipid domains and leakiness of the liposomes. This is followed by the slow release of the encapsulated dye during the second (nearly a single exponential) phase. The experimental data could be best fitted by a two step sequential model (see Discussion), with fast (k_1) and slow (k_2) rate constants of 0.25 ± 0.018 and 0.040 ± 0.0024 min^{-1}, respectively. Of these, the fast rate constant (k_1) corresponds to the single exponential rate constant for the photocleavage of free Glu-lipid (0.32–0.36 min^{-1}; Fig. 2). The slow rate constant (k_2) is ascribed to be the measure of the release of the encapsulated (carboxyfluorescein) dye upon destabilization of the liposome. This rate is about one order of magnitude lower than the rate of the preceding photocleavage step. The fluorescence signal obtained during these experiments is due to the release of carboxyfluorescein. The photocleavage of the lipids and the destabilization of liposomal domains do not yield any fluorescence signal, and thus are manifested in the lag phase.

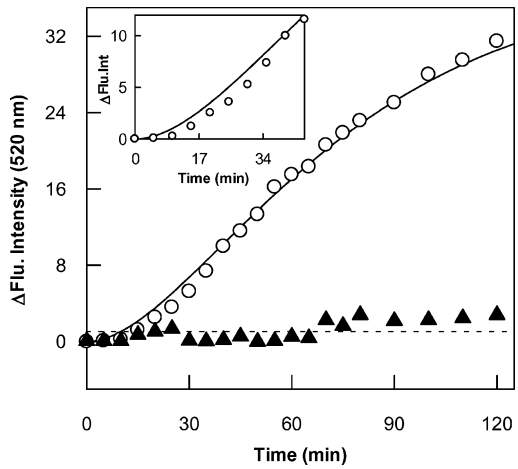

Fig. 5 Kinetic profiles for the release of carboxyfluorescein upon irradiation of liposomes containing Lys-lipid. The increase in fluorescence intensity (ΔF_{518}/nm; λ_{exc} = 495 nm) as a function of time upon irradiation of liposomes (open circles) and when they are kept in the dark (control experiment; filled triangles) are shown. The inset shows an expansion of the data at the initial time scale to show the initial lag phase. The solid smooth line is the best fit of the data for a two-step release of the liposomal content according to eqn. 2, with k_1 and k_2 values of 0.026 ± 0.0037 and 0.025 ± 0.0033 min^{-1}, respectively.

We performed a control experiment to determine the extent to which carboxyfluorescein is bleached during the course of photocleavage of liposomes and their content release. This was important since the amplitude of the fluorescence signal (due to release of the dye from the liposomal lumen) would be affected by the rate as well as the magnitude of photobleaching of the reporter dye. However, when we performed such an experiment under the experimental conditions of Fig. 4, we did not observe any significant photobleaching of carboxyfluorescein (data not shown), which could be envisaged to interfere in assessing the amplitude of fluorescence changes during the course of the photocleavage of Glu-lipid and unloading of the liposome encapsulated dye. Hence, our overall mechanistic conclusion for the release of the liposomal content *via* a "two-step" pathway is not affected by a potential artifact due to photobleaching of the reporter dye.

Since the photocleavage of Lys-lipid was not as efficient as that of Glu- and Asp-lipids (see Figs. 2 and 3), it was of interest to investigate as to how the liposomes formulated by the former lipid would photorelease their encapsulated contents. Toward this goal, we formulated Lys-lipid containing liposomes and encapsulated carboxyfluorescein as a reporter dye as described earlier. As observed with Glu-lipid-containing liposomes, upon irradiation of these liposomes (albeit at 254 nm, since Lys-lipid is not easily photocleaved at 365 nm), there was a time dependent increase in fluorescence at 520 nm ($\lambda_{exc} = 495$ nm). Fig. 5 shows the kinetic profile for the release of carboxyfluorescein as a function of the irradiation time of the liposomes (open circles). We also performed a control experiment in which liposomes were not irradiated (filled triangles). Since the control experiment did not produce any increase in fluorescence, it implied (also as observed in the case of Glu-lipid formulated liposomes) that the unloading of carboxyfluorescein was as a consequence of irradiation of the liposomes, which resulted in the photocleavage of the liposome resident Lys-lipid.

An explicit feature of the kinetic data of Fig. 5 has been the preponderance of the "lag phase", and the latter is more pronounced upon magnifying the initial time scale data points (see the inset of Fig. 5). This is presumably due to the fact that the rate of photocleavage of Lys-lipid ($k = 0.05$–0.08 min^{-1}) is considerably slower than that of Glu- and Asp-lipids ($k = 0.32$ to 0.45 min^{-1}). On assumption that the mechanistic pathway for the photocleavage of liposomes and their content release remains unaffected by the nature of the photocleavable lipids, we analyzed the data of Fig. 5 by a two-step mechanism of eqn. 2. The solid smooth line is the best fit of the data for the k_1 and k_2 values of 0.026 ± 0.0037 and 0.025 ± 0.0033 min^{-1}, respectively. Note that, unlike the photocleavage of Glu- and Asp-lipid formulated liposomes and their content release, the magnitudes of k_1 and k_2 are nearly identical. However, it should be pointed out that these values have been derived from the two distinct kinetic features, *i.e.*, lag and exponential phases, and thus they are not due to apparent artifacts encountered in fitting the kinetic data (comprised of either increasing or decreasing signals) by single exponential *versus* biphasic rate equations.

Irrespectively, it is noteworthy that the magnitude of k_1 (0.026 min^{-1}), derived from the photocleavage of Lys-lipid containing liposomes (Fig. 5), is comparable to the rate constant for the photocleavage of Lys-lipid ($k = 0.05$–0.08 min^{-1}). These values are about one order of magnitude lower than those obtained with Glu-lipid and its associated liposomes. On the other hand, the magnitude of k_2 is similar irrespective of whether the liposome is formulated with Glu-lipid ($k_2 = 0.04$ min^{-1}) or Lys-lipid ($k_2 = 0.025$ min^{-1}). Given these observations, it is tempting to propose that the photocleavage of the *o*-nitrobenzyl conjugated (acidic as well as basic) lipids occur during the lag phase. Since the photocleavage reaction is more facile with Glu-lipid than Lys-lipid, the magnitude of k_1 is about one order of magnitude higher with liposomes formulated with Glu-lipid than with Lys-lipid. But once the liposomes are photocleaved, the release of their content (*i.e.*, carboxyfluorescein as reporter dye) is not dependent (as reflected in similar k_2 values) on the type of amino acid head group utilized to formulate the liposomes.

Discussion

The *o*-nitrobenzyl group-containing lipids exhibited a major absorption peak (predominantly contributed by the aromatic ring) around 250 nm, and a trailing shoulder peak at 300 nm. Although it has been known that substitution at the *o*-nitrobenzyl ring alters its spectral profile, there has been no precedence (to the best of our knowledge) of the distal (side chain) groups of the amino acids influencing the spectral profiles of the chromophore. This is important since all amino acids differ only with respect to their side chain groups, and those groups are far removed from the aromatic ring to exhibit any inductive and/or resonance effects. The question arises how acidic (Glu/Asp) and basic (Lys) amino acid containing photocleavable lipids exhibit different spectral and rate profiles during the course of the cleavage reaction. However, before attempting to answer this question, let us consider a general sequence of steps intrinsic to the photocleavage of *o*-nitrobenzyl group-containing lipids (Scheme 2).

Based on the literature data,[13] it is surmised that upon absorption of the UV light, anionic radical species are generated on the excited nitro group (compound **8**, Scheme 2), which abstracts a benzylic proton and isomerizes to a metastable *aci*-nitro intermediate (compound **9**).[14] The latter is rearranged to yield the nitroso aminol derivative (compound **10**). This is followed by the hydrolysis of the aminol intermediate as the slowest step in the overall photocleavage process.[15] Since the absorption spectra

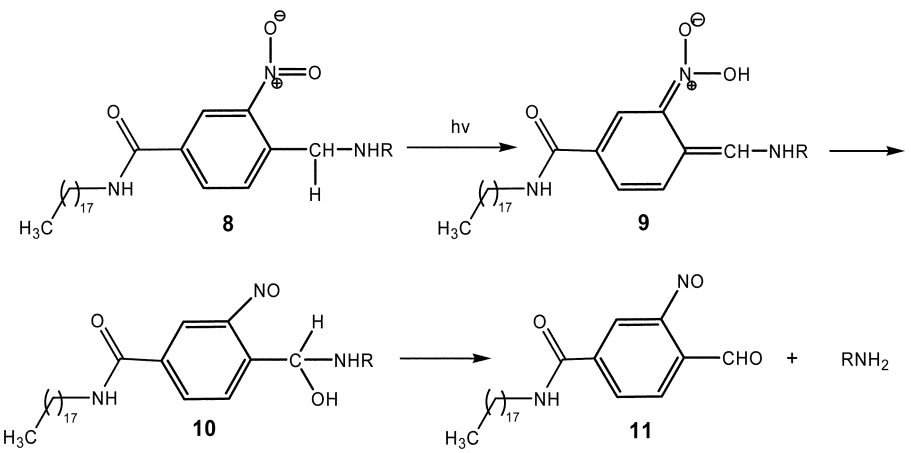

Scheme 2 The proposed sequence of steps during the photocleavage of *o*-nitrobenzyl conjugated lipids.

during the photocleavage of Asp/Glu-lipid are markedly different than those of Lys-lipid, it follows that the side chain groups of the amino acids are responsible for influencing the electronic structures of either the corresponding precursors (compound **8**) or the intermediates (compounds **9** and **10**), but not the final product (compound **11**), as the latter is already devoid of amino acids. Of these, the electronic structural effect is most likely to be manifested at the level of compound **10** or its subsequent derivative(s) (see Scheme 3). At a neutral pH, the side chain groups of Asp/Glu and Lys would predominate as $-COO^-$ and $-NH_3^+$ species, respectively. Of these, the $-NH_3^+$ group of Lys has the potential to interact with either nitroso oxygen (panel A of Scheme 3) or the amide oxygen (panel B of Scheme 3) of compound **10**. Such interactions are expected to facilitate the deprotonation (due to a decrease in the pK_a value) of the aminol carbon atom, resulting in the formation of compounds **12** and **13**, respectively (Scheme 3).

Due to their conjugated nature, both compounds **12** and **13** can yield the red-shifted absorption spectra, albeit they are expected to be more pronounced with compound **13** than with compound **12**. To differentiate which of the above compounds would be more energetically stable, we performed the energy minimizations (ref. 24, employing the semiempirical force field PM3) of intermediates **12** and **13**. This endeavour led to the suggestion that compound **13** was more stable than compound **12**. Hence, the absorption spectra during the course of the photocleavage of Lys-lipid is likely to be dominated at least by the partial accumulation of the intermediate **13**. Therefore, we propose that, although the photocleavage of both Asp/Glu and Lys-lipids predominantly removes the corresponding amino acids (Scheme 2), a minor fraction of the intermediate (particularly in the case of Lys-lipid) is transformed into **13**, and this process is responsible for red shifted spectral profiles during the course of photocleavage of Lys-lipid.

Based on the above discussion, it should not be envisaged that the observed spectral changes Figs. 2 and 3 are primarily dominated by the precursor "nitro" and the product "nitroso" derivatives.[14,15,25] Although other chromophoric intermediates are likely to form during the photocleavage of *o*-nitrobenzyl conjugates, they are not detectable due to their shorter lifetimes.

Another interesting aspect of photocleavage is the fact that the rate constant for the cleavage of Glu/Asp-lipid is about one order of magnitude higher that of the Lys-lipid (Figs. 2 and 3). This is besides the fact that the photocleavage of Lys-lipid requires a higher energy (254 nm) UV source than Glu/Asp-lipid; the latter lipids are cleaved even upon irradiation with a 365 nm UV source. We think that the origin of both these features lays in the preferential stabilization of the "precursor" ground state of the Lys-lipid as compared to that of the Glu/Asp lipid. This can occur due to the interaction of the $-NH_3^+$ group of Lys with the amide oxygen of the precursor (compound **8**, Scheme 2), essentially *via* the same mechanism involved in yielding the red-shifted absorption spectra during the photocleavage of Lys-lipid (Scheme 2). Hence, although the overall microscopic pathways for the photocleavage of different amino acid containing lipids can be the same, their spectral and kinetic profiles can be significantly different. Therefore, detailed mechanistic studies for the overall photocleavage reaction of *o*-nitrobenzyl group-containing amino-lipid conjugates are essential for designing liposomes as efficient drug delivery vehicles.

The release of the liposome-encapsulated carboxyfluorescein upon irradiation can be envisaged to be the product of two microscopic events: the first involving the photocleavage of liposome resident *o*-nitrobenzyl conjugated lipids followed by the destabilization of liposomes and release of the encapsulated dye during the second step. These microscopic events are corroborated

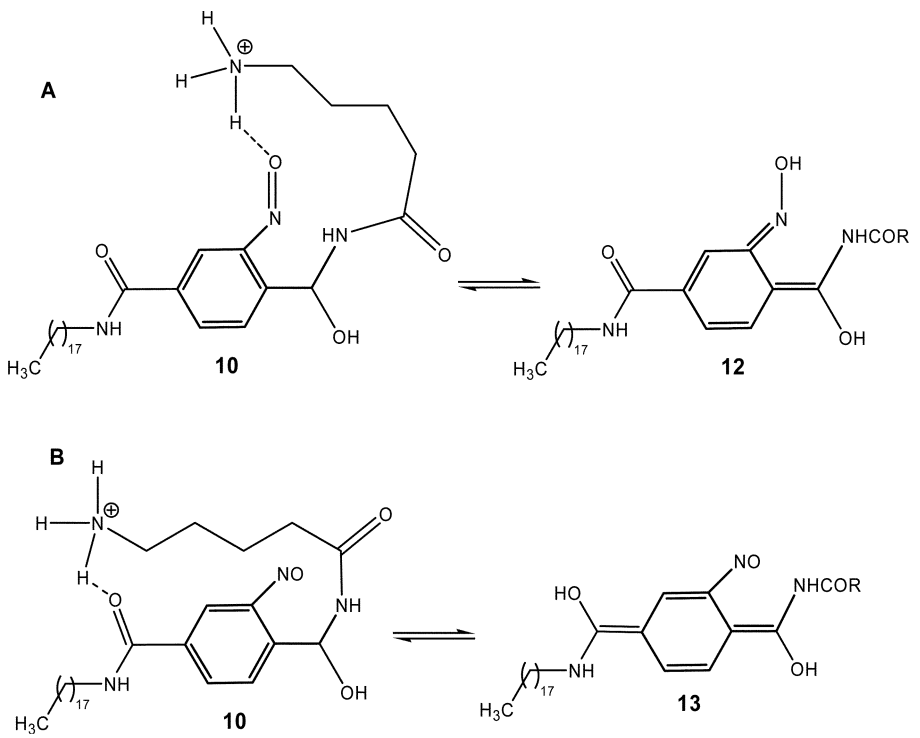

Scheme 3 Alternative modes of binding of the side chain group of Lys of compound **10**, and generation of conjugated reaction products.

by the emergence of a "lag" followed by an "exponential" kinetic phase (Figs. 4 and 5) during the course of photocleavage and "unloading" of the liposomal content. The prevalence of the "lag" phase is more explicit on examining the kinetic data at shorter time scales (insets of Figs. 4 and 5). Since the increase in the fluorescence signal of carboxyfluorescein is due to the release of the dye from photocleaved liposomes, and not due to the photocleavage event *per se*, the latter process can be easily manifested in the "lag" phase in the experimental conditions of Figs. 4 and 5. A cumulative account of the experimental data leads us to propose a "two-step" minimal model for the photocleavage of liposomes and unloading of their contents (eqn. 1).

$$L - F \xrightarrow{k_1} L^* - F \xrightarrow{k_2} L^* + F \qquad (1)$$

Here, L and F represent liposomes and carboxyfluorescein, respectively. The first step involves the photocleavage of the *o*-nitrobenzyl conjugated lipids, incorporated in the liposomes, leading to destabilization of the liposomes. The intermediary species L*–F is representative of the photocleaved liposomes, with fluorescence dye still entrapped in their lumen. The second step is the release of the fluorescence dye with a concomitant increase in the fluorescence emission intensity at 520 nm. For this irreversible two step model, the time course of formation of free carboxyfluorescein (F) can be given by equation 2.

$$F = [L - F]\left[1 + \left(\frac{1}{k_1 - k_2}\right)\{k_2 \exp(-k_1 t) - k_1 \exp(-k_2 t)\}\right] \qquad (2)$$

It should be mentioned that eqn. 2 has been explicitly derived by Frost and Pearson,[26] and has been utilized extensively for analyzing the kinetic data of "two-step" irreversible reactions such as that given by eqn. 1. The kinetic data of Figs. 4 and 5 could be easily analyzed by eqn. 2, yielding the k_1 and k_2 values intrinsic to the photocleavage of differently formulated liposomes and releasing their contents. Of derived kinetic parameters (from the best fit of the experimental data), it is apparent that the k_1 value matches the single exponential rate constant for the photocleavage of the corresponding lipid. For example, k_1 is about one order of magnitude higher for Glu-lipid ($k_1 = 0.25\ min^{-1}$) than for Lys-lipid ($k_1 = 0.026\ min^{-1}$) since the rate of photocleavage of the former lipid ($k = 0.32$–$0.36\ min^{-1}$; Fig. 2) is about one order of magnitude faster than that of the latter lipid ($k = 0.05$–$0.08\ min^{-1}$; Fig. 3). On the other hand, the magnitude of k_2 is not affected by the type of lipid utilized to formulate liposomes. For example, the k_2 values derived from photocleavage and unloading of encapsulated dye are similar for Glu-lipid ($0.04\ min^{-1}$) and Lys-lipid ($0.025\ min^{-1}$). Clearly, once the liposome resident lipids are cleaved, the release of encapsulated dye is dominated by some common molecular mechanism, and that mechanism is likely to be the organization of the liposomal domains (after the photocleavage of the polar head group). We surmise that the organization of the lipid domains serves as the rate-limiting step for unloading its contents to exterior media. We are currently in the process of testing this hypothesis by formulating different types of liposomes, and we will report these findings subsequently.

Conclusions

The experimental data presented herein lead to the following conclusions: (1) Photocleavable lipids can be easily synthesized by bridging a C_{18} chain fatty acid (non-polar group) and Glu, Asp, and Lys as charged amino acids (as polar groups) with an *o*-nitrobenzyl moiety. (2) Although all the charged amino acid head groups can be utilized to formulate liposomes, the Glu/Asp-lipid-harboring liposomes are more easily cleaved than Lys-lipid lipid-harboring liposomes. (3) The photocleavage of liposomes and the release of their contents proceed *via* a two-step mechanism, of which the feasibility of the first (photocleavage) step is dependent on whether the amino acid (forming the head group) is acidic or basic in nature. The second (rate limiting) step is dictated by the organization of the lipid domains following the separation of the amino acid head groups. The insight gained from these studies will serve as the prototype for formulating photocleavable liposomes and using them as drug delivery vehicles for treating different types of diseases.

Experimental

Commercial reagents were purchased from either Aldrich or Acros Chemical Co. The protected amino acids were purchased from Nova Biochem. Nitric acid (90%) was from Alfa Aesar. All solvents used for reactions were analytical grade and were used without further purification. Melting points were determined on a micro melting point apparatus. ^1H and ^{13}C NMR spectra were recorded using 300, 400 or 500 MHz spectrometers.

Solvents used for NMR were one of the following: $CDCl_3$, CD_3OD or DMSO-d_6 with TMS as the internal standard. Elemental analyses were obtained from facilities at Desert Analytics (Tucson, AZ). TLC was performed with Adsorbosil plus IP, 20 × 20 cm plate, 0.25 mm (Altech Associates, Inc.). Chromatography plates were visualized by either UV light or in an iodine chamber. For drying water-wet compounds, lyophilization (Freeze Dry system/Freezone 4.5; Labconco) was used. Reactions were performed either under an N_2 atmosphere or using a guard tube. For extractive workups, the organic layer was dried over anhydrous Na_2SO_4, and concentrated *in vacuo.*

3-Nitro-4-(trifluoroacetylaminomethyl)benzoic acid (2)

Trifluoroacetic anhydride (5.9 mL, 41.3 mmol) was added in small portions to solid 4-(aminomethyl) benzoic acid (2.5 g, 16.5 mmol) at 4 °C. Upon completion of addition, the reaction mixture was homogeneous. Stirring was continued at 25 °C for 2 h, and then ice–water was added to precipitate the product. The white solid was collected by filtration, washed with water and dried. Yield: 3.63 g (88%), mp: 199–203 °C; ^1H NMR δ_H (300 MHz; $CDCl_3$; 293 K; Me_4Si) 7.91 (d, *J* 7.8, 2H, ArH), 7.37 (d, *J* 7.8, 2H, ArH), 4.44 (s, 2H, $ArCH_2$).

The above compound (3.63 g, 14.7 mmol) was added over 1 h to 90% nitric acid (20 mL) at −10 °C. The mixture was stirred further for 1.5 h at 0 °C and then poured onto ice to precipitate the product. The precipitated solid was filtered, washed with plenty of water to neutral pH, and lyophilized to provide an off-white solid (3.95 g, 92%), mp: 210–211 °C; ^1H NMR δ_H (300 MHz; $CDCl_3$;

298 K; Me_4Si) 8.61 (d, *J* 1.6, 1H, ArH), 8.17 (dd, *J* 1.6, 8.1, 1H, ArH), 7.51 (d, *J* 8.1 Hz, 1H, ArH), 4.74 (s, 2H, $ArCH_2$).

4-(Boc-aminomethyl)-3-nitrobenzoic acid (3)

According to a general procedure,[27] a solution of compound **2** (0.68 g, 2.3 mmol) and K_2CO_3 (0.81 g, 5.8 mmol) in MeOH–H_2O (1 : 1, 16 mL) was maintained at 25 °C for 10 h. The dark yellow solution was concentrated under reduced pressure, and the resultant solid was dissolved in dioxane–H_2O (1 : 1, 10 mL). Di-*tert*-butyl dicarbonate (0.77 g, 3.5 mmol) was added, and after 2.5 h, the reaction mixture was concentrated *in vacuo.* Ether and water were added, and the aqueous phase was washed with ether, the pH was adjusted to 3.0 with 10% aqueous citric acid, and extracted with ethyl acetate. The combined ethyl acetate phases were washed with brine, dried over Na_2SO_4, and concentrated *in vacuo* to give the title product as a yellow solid (0.67 g, 97%), mp 124–126 °C; ^{1}H NMR δ_H (300 MHz; $CDCl_3$; 298 K; Me_4Si) 8.74 (d, *J* 1.6, 1H, ArH), 8.30 (dd, *J* 1.6, 8.0, 1H, ArH), 7.77 (d, *J* 8.0, 1H, ArH), 4.65 (s, 2H, $ArCH_2$), 1.44 (s, 9H, t-butyl CH_3).

***N*-Stearyl-4-(aminomethyl)-3-nitrobenzamide (4)**

Compound **3** (0.8 g, 2.7 mmol) was dissolved in $CHCl_3$ (20 mL) and stearic acid (0.71 g, 2.7 mmol), HOBT (0.364 g, 2.7 mmol), HBTU (1.024 g, 2.7 mmol) and Et_3N (0.75 mL, 5.4 mmol) were added to the solution. The mixture was stirred at room temperature for 10 h. The reaction mixture was then washed with water; the organic phase dried and solvent was removed *in vacuo.* The residue was purified by column chromatography (eluant: 5% methanol in chloroform, $R_f = 0.3$) to obtain the pure product as a yellow solid (1.19 g, 81%), mp: 84–86 °C; ^{1}H NMR δ_H (300 MHz; $CDCl_3$; 298 K, Me_4Si) 8.41 (d, *J* 1.8, 1H, ArH), 8.00 (dd, *J* 1.8, 8.1, 1H, ArH), 7.68 (d, *J* 8.1, 1H, ArH), 6.41 (br s, 1H, CONH), 5.30 (br s, 2H, NH_2), 4.59 (s, 2H, $ArCH_2$), 3.45 (q, *J* 6.9, 2H, $CONHCH_2$), 1.65–1.57 (m, 2H, $CONHCH_2CH_2$), 1.42 (s, 9H, t-butyl CH_3), 1.24–1.33 (m, 30H, stearyl CH_2), 0.87 (t, *J* 6.9, 3H, stearyl CH_3).

To the above compound (1.16 g, 2.12 mmol), was added, 4 M HCl in dioxane (8 mL) and the reaction mixture was stirred at room temperature for 3 h. The solvent was then removed under vacuum and water added to the residue. The insoluble white solid was filtered, washed with plenty of water and dried to give compound **4** (0.89 g, 94%) as a yellow solid. The compound was carried on to the next step without further purification. ^{1}H NMR δ_H (300 MHz; $CDCl_3$; 298 K, Me_4Si) 8.54 (d, *J* 1.8, 1H, ArH), 8.03 (dd, *J* 1.8, 7.5, 1H, ArH), 7.75 (d, *J* 7.5, 1H, ArH), 4.31 (s, 2H, $ArCH_2$), 3.31 (q, *J* 6.9, 2H, $CONHCH_2$), 1.53–1.49 (m, 2H, $CONHCH_2CH_2$), 1.40–1.12 (m, 30H, stearyl CH_2), 0.78 (t, *J* 7, 3H, stearyl CH_3).

3-*t*-Butoxycarbonylamino-*N*-(2-nitro-4-octadecylcarbamoylbenzyl)succinamic acid *t*-butyl ester (5)

Compound **4** (0.3 g, 0.67 mmol), Boc-Asp(O^tBu)–OH dicyclohexylamine salt (0.32 g, 0.67 mmol), HOBT (0.091 g, 0.67 mmol) and HBTU (0.25 g, 0.67 mmol) were taken up in DMF (15 mL) and *N*-methylmorpholine (0.15 mL, 1.34 mmol) was added. The reaction mixture was stirred at room temperature overnight. The solvent was removed *in vacuo*. Water was added to the residue and extracted with ethyl acetate. The ethyl acetate layer was dried (Na_2SO_4) and solvent was removed by rotary evaporation. The crude product was purified by silica gel chromatography (eluant: $CHCl_3$, $R_f = 0.2$) to yield compound **5** as a white solid (0.480 g, 99%), mp: 90–92 °C; ^{1}H NMR δ_H (300 MHz; $CDCl_3$; 298 K, Me_4Si) 8.41 (d, *J* 1.6, 1H, ArH), 7.98 (dd, *J* 1.6, 8.0, 1H, ArH), 7.70 (d, *J* 8.0, 1H, ArH), 4.82–4.70 (m, 2H, $ArCH_2$), 4.51–4.44 (m, 1H, COCH), 3.47 (q, *J* 7, 2H, $CONHCH_2$), 2.96–2.88 (m, 1H, $CH_2CO_2Bu^t$), 2.62–2.58 (m, 1H, $CH_2CO_2Bu^t$), 1.66–1.58 (m, 2H, $CONHCH_2CH_2$), 1.45 (s, 9H, ester t-butyl CH_3), 1.42 (s, 9H, carbamate t-butyl CH_3), 1.40–1.20 (m, 30H, stearyl CH_2), 0.88 (t, *J* 7.0, 3H, stearyl CH_3).

4-*t*-Butoxycarbonylamino-4-(2-nitro-4-octadecylcarbamoylbenzylcarbamoyl)butyric acid *t*-butyl ester (6)

Compound **4** (0.3 g, 0.67 mmol), Boc-Glu(O^tBu)–OH (0.2 g, 0.67 mmol), HOBT (0.09 g, 0.67 mmol) and HBTU (0.25 g, 0.67 mmol) were taken up in DMF (15 mL) and *N*-methylmorpholine (0.15 mL, 1.34 mmol) was added. The reaction mixture was stirred at room temperature overnight. The work-up procedure was the same as described for compound **5**. The crude product was then purified by silica gel chromatography (eluant: $CHCl_3$, $R_f = 0.3$) to provide the glutamic acid derivative **6** as a yellow solid. Yield: 0.34 g (70%); ^{1}H NMR δ_H (300 MHz; $CDCl_3$; 298 K, Me_4Si) 8.42 (d, *J* 1.6, 1H, ArH), 8.98 (dd, *J* 1.6, 8.0, 1H, ArH), 7.71 (d, *J* 8.0, 1H, ArH), 4.75 (d, *J* 6, 2H, $ArCH_2$), 4.15–4.08 (m, 1H, COCH), 3.47 (q, *J* 7, 2H, $NHCH_2$), 2.43–2.37 (m, 1H, $CH_2CH_2CO_2Bu^t$), 2.31–2.25 (m, 1H, $CH_2CH_2CO_2Bu^t$), 2.11–2.02 (m, 1H, $CH_2CH_2CO_2Bu^t$), 1.95–1.87 (m, 1H, $CH_2CH_2CO_2Bu^t$), 1.65–1.6 (m, 2H, $NHCH_2CH_2$), 1.45 (s, 9H, ester t-butyl CH_3), 1.42 (s, 9H, carbamate t-butyl CH_3), 1.40–1.20 (m, 30H, stearyl CH_2), 0.88 (t, *J* 7.0, 3H, stearyl CH_3).

[5-*t*-Butoxycarbonylamino-1-(2-nitro-4-ocatdecylcarbamoylbenzylcarbamoyl)pentyl]carbamic acid *t*-butyl ester (7)

Compound **4** (0.3 g, 0.67 mmol), Boc-Lys(Boc)–OH (0.22 g, 0.67 mmol), HOBT (0.09 g, 0.67 mmol) and HBTU (0.25 g, 0.67 mmol) were taken up in DMF (15 mL) and *N*-methylmorpholine (0.15 mL, 1.34 mmol) was added. The work-up procedure was the same as described for compound **5**. The crude product was purified by silica gel chromatography (eluant: 2% MeOH in $CHCl_3$, $R_f = 0.2$) to yield the lysine derivative **7** as a white foamy solid. Yield: 0.45 g (87%); ^{1}H NMR δ_H (500 MHz; $CDCl_3$; 298 K, Me_4Si) 8.38 (d, *J* 1.6, 1H, ArH), 7.96 (dd, *J* 1.6, 8.0, 1H, ArH), 7.62 (d, *J* 8.0, 1H, ArH), 4.76–4.64 (m, 2H, $ArCH_2$), 4.66–4.63 (m, 1H, COCH), 3.43 (q, *J* 7, 2H, $NHCH_2$), 3.02–2.95 (m, 2H, CH_2NHBoc), 1.82–1.72 (m, 2H, lysine CH_2) 1.66–1.58 (m, 2H, $NHCH_2CH_2$), 1.43 (s, 9H, t-butyl CH_3), 1.40 (s, 9H, t-butyl CH_3), 1.39–1.35 (m, 4H, lysine CH_2), 1.35–1.15 (m, 30H, stearyl CH_2), 0.87 (t, *J* 7.2, 3H, stearyl CH_3).

3-Amino-*N*-(2-nitro-4-octadecylcarbamoyl-benzyl)-succinamic acid (Asp-lipid)

To the Boc-Asp(O^tBu) derivative **5** (0.40 g, 0.56 mmol), was added 4 mL of trifluoroacetic acid and a drop of anisole. The reaction mixture was stirred at room temperature for two hours. It was then slowly added to water and aqueous NaOH solution

(1 M) was slowly added to neutralize the TFA. The precipitate was collected by filtration, washed with plenty of water and dried to give Asp-lipid as a off-white solid (0.27 g, 85%); mp: 154–157 °C; ^{1}H NMR δ_H (400 MHz; d_6-DMSO; 298 K, Me_4Si, without exchangeable protons) 8.43 (d, *J* 1.6, 1H, ArH), 8.10 (dd, *J* 1.6, 8.0, 1H, ArH), 7.62 (d, *J* 8.0, 1H, ArH), 4.66–4.56 (m, 2H, $ArCH_2$), 3.96–3.92 (m, 1H, COCH), 3.24 (q, *J* 7, 2H, $NHCH_2$), 2.75–2.58 (m, 2H, CH_2CO_2H), 1.60–1.40 (m, 2H, $NHCH_2CH_2$), 1.35–1.17 (m, 30H, stearyl CH_2), 0.82 (t, *J* 7.0, 3H, stearyl CH_3); ^{13}C NMR δ_C (100 MHz; d_6-DMSO; 298 K) 176.05, 171.99, 64.42, 148.52, 136.77, 135.50, 132.54, 130.66, 123.81, 50.71, 37.19, 31.87, 30.38, 29.58–29.23, 27.10, 22.64, 14.45. Anal. Calcd. for $C_{30}H_{50}N_4O_6.3CF_3COONa.4H_2O$: C, 41.46; H, 5.61; N, 5.37. Found: C, 41.25; H, 5.92; N, 5.43%.

4-Amino-4-(2-nitro-4-octadecylcarbamoylbenzylcarbamoyl)butyric acid (Glu-Lipid)

To the Boc-Glu(O^{t}Bu) derivative **6** (0.26 g, 0.36 mmol), was added 4 mL of trifluoroacetic acid and a drop of anisole. The reaction mixture was stirred at room temperature for 2 h. The work-up procedure was the same as described for Asp-lipid. Glu-lipid was isolated as a white solid (0.2 g, 99%); mp: 150–152 °C; ^{1}H NMR δ_H (400 MHz; d_6-DMSO; 298 K, Me_4Si, exchangeable protons not reported) 8.49 (d, *J* 1.6, 1H, ArH), 8.14 (dd, *J* 1.6, 8.0, 1H, ArH), 7.64 (d, *J* 8.0, 1H, ArH), 4.70–4.62 (m, 2H, $ArCH_2$), 3.92–3.84 (m, 1H, COCH), 3.24 (q, *J* 7, 2H, $NHCH_2$), 2.36–2.22 (m, 2H, $CH_2CH_2CO_2H$), 1.99–1.90 (m, 2H, $CH_2CH_2CO_2H$), 1.58–1.40 (m, 2H, $NHCH_2CH_2$), 1.35–1.10 (m, 30H, stearyl CH_2), 0.82 (t, *J* 7.0, 3H, stearyl CH_3); ^{13}C NMR δ_C (100 MHz; d_6-DMSO; 298 K) 176.02, 169.43, 165.68, 147.94, 135.73, 135.38, 132.15, 130.50, 124.08, 52.69, 40.97, 40.47, 31.96, 30.38, 29.73–29.38, 27.13, 26.72, 22.70, 14.03. Anal. Calcd. for $C_{31}H_{52}N_4O_6.CF_3COONa.H_2O$: C, 55.61; H, 7.85; N, 7.86. Found: C, 55.27; H, 8.07; N, 8.02%.

4-[(2,6-Diaminohexanoylamino)methyl]-3-nitro-*N*-octadecyl benzamide (Lys-lipid)

To the di-Boc-lysine derivative **7** (0.38 g, 0.49 mmol), were added 4 mL of trifluoroacetic acid and a drop of anisole. The reaction mixture was stirred at room temperature for 2 h. The work-up procedure was the same as described for Asp-lipid. Lys-lipid was obtained as a light yellow solid (0.28 g, quantitative); mp: 130–134 °C; ^{1}H NMR δ_H (400 MHz; d_6-DMSO; 298 K, Me_4Si, exchangeable protons not reported) 8.35 (d, *J* 1.6, 1H, ArH), 7.89 (dd, *J* 1.6, 8.0, 1H, ArH), 7.48 (d, *J* 8.0, 1H, ArH), 4.58–4.48 (m, 3H, ArCH2 and COCH), 3.25 (q, 7.2, 2H, $NHCH_2$), 3.21–3.18 (m, 2H, lysine CH_2NH_2), 2.50 (t, *J* 6.8, 2H, lysine CH_2), 1.62–1.54 (m, 2H, $NHCH_2CH_2$), 1.50–1.42 (m, 2H, lysine CH_2), 1.41–1.15 (m, 2H, lysine CH_2), 1.15–1.07 (m, 30H, stearyl CH_2), 0.73 (t, *J* 7.2, 3H, stearyl CH_3); ^{13}C NMR δ_C (100 MHz; d_6-DMSO; 298 K) 176.63, 164.37, 148.39, 137.97, 135.02, 132.51, 130.30, 123.85, 55.48, 42.01, 35.60, 31.94, 29.66–29.35, 27.11, 23.35, 22.74, 14.58. Anal. Calcd. for $C_{32}H_{57}N_5O_4.2CF_3COOH.H_2O$: C, 52.61; H, 7.48; N, 8.52. Found: C, 52.37; H, 7.08; N, 8.37%.

Preparation of carboxyfluorescein-encapsulated liposomes

The photocleavable lipid (0.45 μmoles, 5 mol%) and solid 1,2-distearoyl-sn-glycero-3-phosphocholine (6.716 mg, 8.55 μmoles, 95 mol%) were dissolved in 5 mL of anhydrous chloroform and 500 μL of anhydrous methanol in a 25 mL clean, oven-dried round bottomed flask. The organic solvents were then removed in a rotary evaporator under reduced pressure maintaining the bath temperature at 40 °C until a thin and uniform lipid film was formed on the walls of the round-bottomed flask. The flask was left on the rotary evaporator for an additional 15 minutes and then allowed to dry *in vacuo* for 20 hours.

In another clean dry glass vial, 56 mg (150 μmoles) of 6-carboxyfluorescein was taken up in 3 mL of HEPES buffer (25 mM, pH = 7.0). The dye was dissolved by first bath-sonicating (to reduce the particle size of the solid granules of the dye) to form a dark brown transparent solution. The thin dry lipid film was then hydrated with the dye solution (3 mL) by rotating slowly in the rotary evaporator bath at 60 °C for 1 hour. The resulting suspension was then subjected to probe sonication (power: 50 W) at 60 °C for 1 hour with constant nitrogen bubbling, to get a clear dark red liposome solution. The total lipid concentration was 9 mM. The osmolarity of the liposome solution was measured with a standard micro osmometer.

Sephadex G-50 resin (particle size 50–150 μm) was mixed with an excess of water to form a gel and the gel was hydrated overnight at 40 °C in the water bath of a regular rotary evaporator. A chromatography column was packed with the gel after cooling to room temperature and equilibrated with 200 mL of water whose osmolarity was made equal to that of the liposome solution by the addition of solid sodium chloride. The liposome solution was then loaded on top of the column and slowly eluted. The liposomes came out first as a yellow non-fluorescent solution and were collected.

Uncorking of liposomes and their content release

The fluorescence emission spectrum of the dye-encapsulated liposomes was recorded with excitation at 580 nm. The quartz cuvet was then placed under a UV lamp (100 W lamp for the 365 nm irradiation for liposomes incorporating Asp-lipid and Glu-lipid; 10 W lamp for 254 nm irradiation for liposomes incorporating Lys-lipid; distance from the lamp: 5 cm; area of illumination: 1 cm × 1 cm). Every 5 minutes, the cuvet was transferred to the fluorimeter and the emission spectrum was recorded. The intensity of the emission maximum (518 nm) was plotted as a function of time to generate the release curves for the dye-encapsulated liposomes.

Acknowledgements

This research was supported by the National Institutes of Health grants 1R15 DK56681-01A1 to D. K. S. and 1P20 RR 15566-01 to S. M.

References

1 V. P. Torchilin, *Nat. Rev. Cancer*, 2005, **4**, 145–160.
2 D. Ppahadjopous, in *Liposomes: Rational Design*, ed. A. S. Janoff, Marcel Dekker, New York, 1999, pp. 1–12; T. Ishida, H. Harashima and H. Kiwada, *Biosci. Rep.*, 2002, **22**, 197–224.
3 R. J. Banerjee, *J. Biomater. Appl.*, 2001, **16**, 3–21.
4 A. S. L. Derycke and P. A. M. de Witte, *Adv. Drug. Delivery Rev.*, 2004, **56**, 17–30.

5 H. M. Lee and J. Chmielewski, *J. Pept. Res.*, 2005, **65**, 355–363; T. L. Andresen, S. S. Jensen and K. Jorgensen, *Prog. Lipid Res.*, 2005, **44**, 68–97.
6 S. L. Huang and R. C. MacDonald, *Biochim. Biophys. Acta*, 2004, **1665**, 134–141; N. Karoonuthaisiri, K. Titiyevskiy and J. L. Thomas, *Colloids Surf., B*, 2003, **27**, 365–375.
7 S. C. Davis and F. C. Szoka, *Bioconjugate Chem.*, 1998, **9**, 783–792.
8 H. D. Han, T. W. Kim, B. C. Shin and H. S. Choi, *Macromol. Res.*, 2005, **13**, 54–61; K. Yoshino, A. Kadowaki, T. Takagishi and K. Kono, *Bioconjugate Chem.*, 2004, **15**, 1102–1109.
9 Z. Li, Y. Wan and A. G. Kutateladze, *Langmuir*, 2003, **19**, 6381–6391; Y. Wan, J. K. Angleson and A. G. Kutateladze, *J. Am. Chem. Soc.*, 2002, **124**, 5610–5611; T. Spratt, B. Bondurant and D. F. O'Brien, *Biochim. Biophys. Acta*, 2003, **1611**, 35–43. For photo-polymerization induced liposomal leakage, see: A. Mueller and D. F. O'Brien, *Chem. Rev.*, 2002, **102**, 727–757.
10 T. L. Anderson, J. Davidsen, M. Begtrup, O. G. Mouritsen and K. Jorgensen, *J. Med. Chem.*, 2004, **47**, 1694–1703; X. Guo and F. C. Szoka, *Acc. Chem. Res.*, 2003, **36**, 335–341; J. Davidsen, K. Jorgensen, T. L. Andersen and O. G. Mouritsen, *Biochim. Biophys. Acta*, 2003, **1609**, 95–101.
11 N. R. Sarkar, T. Rosendahl, A. B. Krueger, A. L. Banerjee, K. Benton, S. Mallik and D. K. Srivastava, *Chem. Commun.*, 2005, 999–1001.
12 M. Egeblad and Z. Werb, *Nat. Rev. Cancer*, 2002, **2**, 161–174.
13 A. Blanc and C. G. Bochet, *J. Am. Chem. Soc.*, 2004, **126**, 7174–7175; M. C. Pirrung, W. H. Pieper, K. P. Kalippan and M. R. Dhananjeyan, *Proc. Natl. Acad. Sci. U. S. A.*, 2003, **100**, 12548–12553; A. Blanc and C. G. Bochet, *J. Org. Chem.*, 2003, **68**, 1138–1141; K. Schaper, S. A. M. Mobarekeh and C. Grewer, *Eur. J. Org. Chem.*, 2002, 1037–1046; R. Wieboldt, D. Ramesh, E. Jabri, P. A. Karplus, B. K. Carpenter and G. P. Hess, *J. Org. Chem.*, 2002, **67**, 8827–8831.
14 Z. Guan, J. T. Roland, J. Z. Bai, S. X. Ma, T. M. McIntire and M. Nguyen, *J. Am. Chem. Soc.*, 2004, **126**, 2058–2065; Y. Luo and M. S. Shoichet, *Biomacromolecules*, 2004, **5**, 2315–2323; C. P. Salerno and H. J. Cleaves, *Synth. Commun.*, 2004, **34**, 2379–2386; C. Dinkel, O. Wichmann and C. Schultz, *Tetrahedron Lett.*, 2003, **44**, 1153–1155; C. G. Bochet, *J. Chem. Soc., Perkin Trans. 1*, 2002, 125–142.
15 T. S. Seo, X. Bai, H. Ruparel, Z. Li, N. J. Turro and J. Ju, *Proc. Natl. Acad. Sci. U. S. A.*, 2004, **101**, 5488–5493; X. Bai, S. Kim, Z. Li, N. J. Turro and J. Ju, *Nucleic Acids Res.*, 2004, **32**, 535–541; Z. Li, X. Bai, H. Ruparel, S. Kim, N. J. Turro and J. Ju, *Proc. Natl. Acad. Sci. U. S. A.*, 2003, **100**, 414–419.
16 Y. V. Il'ichev, M. A. Schwoerer and J. Wirz, *J. Am. Chem. Soc.*, 2004, **126**, 4581–4595; B. V. Zemelman, N. Nesnas, G. A. Lee and G. Miesenbock, *Proc. Natl. Acad. Sci. U. S. A.*, 2003, **100**, 1352–1357; J. E. T. Corrie, A. Barth, V. R. N. Munasinghe, D. R. Trentham and M. C. Hutter, *J. Am. Chem. Soc.*, 2003, **125**, 8546–8554.
17 A. Dussy, C. Meyer, E. Quennet, T. A. Bickle, B. Giese and A. Marx, *ChemBioChem.*, 2002, **3**, 54–60.
18 L. Wang, J. E. T. Corrie and J. F. Wootton, *J. Org. Chem.*, 2002, **67**, 3474–3478.
19 M. Wilcox, R. W. Viola, K. W. Johnson, A. P. Billington, B. K. Carpenter, J. A. McCray, A. P. Guzikowski and G. P. Hess, *J. Org. Chem.*, 1990, **55**, 1585–1589.
20 Z. Zhang, H. Hatta, T. Ito and S. I. Nishimoto, *Org. Biomol. Chem.*, 2005, **3**, 592–596; M. Nomura, S. Shuto and A. Matsuda, *Bioorg. Med. Chem.*, 2003, **11**, 2453–2461; M. P. Hay, G. J. Atwell, W. R. Wilson, S. M. Pullen and W. A. Denny, *J. Med. Chem.*, 2003, **46**, 2456–2466.
21 For preliminary results, see: B. Chandra, S. Mallik and D. K. Srivastava, *Chem. Commun.*, 2005, 3021–3023.
22 T. Nagasaki, A. Taniguchi and S. Tamagaki, *Bioconjugate Chem.*, 2003, **14**, 513–516.
23 H. Komatsu and P. L. G. Chong, *Biochemistry*, 1998, **37**, 107–115.
24 *Spartan 04 for Windows*, Wavefunction Inc., Irvine, CA, USA, 2004.
25 H. Feuer, in *The Chemistry of the Nitro and Nitroso Groups. Part 1*, Interscience Publishers, Wiley and Sons, NY, 1969.
26 A. A. Frost and R. G. Pearson, 1961, *Kinetics and Mechanism*, Wiley, New York.
27 H. Newman, *J. Org. Chem.*, 1965, **30**, 1287–1288.

